Soft Matter

Cite this: *Soft Matter*, 2012, **8**, 7604

www.rsc.org/softmatter

PAPER

Non-linear alignment dynamics in suspensions of platelets under rotating magnetic fields†

Randall M. Erb,[a] Jana Segmehl,[a] Michalis Charilaou,[bc] Jörg F. Löffler[b] and André R. Studart*[a]

Received 21st March 2012, Accepted 17th May 2012
DOI: 10.1039/c2sm25650a

Under rotating magnetic fields, micron-sized platelets suspended in a fluid and decorated with magnetic nanoparticles are found to assume two orientational states. This behavior is very attractive for the development of unusual reinforcement architectures in synthetic composites. However, it is highly dependent on the frequency of the magnetic field and the rheological properties of the fluid. At low frequencies or fluid viscosities, the magnetized platelets continuously rotate in the fluid. At high frequencies and fluid viscosities, a non-linear response is observed in which the platelets align parallel to the plane of the rotating field. In this study we offer a theoretical description and experimental verification of this phenomenon, which can be used to build composites with fully aligned platelet reinforcement.

Introduction

Magnetic fields have been used to manipulate nonmagnetic colloidal particles in suspensions including spheres,[1,2] rods,[3,4] and platelets.[5,6] Typically, to apply a magnetic force to these nonmagnetic particles using low magnetic fields, iron oxide nanoparticles are placed either in the surrounding fluid (negative magnetophoresis) or on the surface of the nonmagnetic particles (magnetic labeling). In both cases, the magnetic nanoparticles attempt to guide the alignment, assembly or transport of the nonmagnetic particles into configurations that have minimal magnetic energy. Using the magnetic nanoparticles as a permeability contrast agent dispenses with the costly and burdensome ultra-high magnetic field setups normally used to manipulate low-susceptibility materials.[7] In addition, by selecting nonmagnetic particles of specific sizes which are not dominated by gravitational or thermal energies, it is possible to use magnetic fields as low as 1 mT for manipulation.

Recently, ultra-high magnetic response (UHMR) was shown in suspensions of anisotropic particles consisting of 7.5 μm-long and 200 nm-thick aluminum oxide platelets coated with 12 nm iron oxide nanoparticles.[5] These platelets were aligned in polymer solutions and liquid monomers, producing a new family of composite structures upon the consolidation of the fluid media. Using this technique, static magnetic fields can only align the platelets in one of their rotational degrees of freedom, allowing rotation in the other two and limiting the maximum volume fraction of platelets in the final composite. Previous studies have shown that rotating fields can be used to fix an additional degree of rotation of the platelets.[8] In this case, the interplay between the rotating magnetic field and the particle suspension generates complex, non-linear dynamics. While at low magnetic-field frequencies the platelets exhibit synchronous rolling motions, biaxial alignment into ordered assemblies is observed at high frequencies. Understanding these dynamics is essential to using these techniques to align particles in a suspension within two orientational axes.

In this study we theoretically describe the transition between synchronous rolling and alignment of the second orientational axis of magnetically labeled platelets on a substrate surface. Our theoretical considerations indicate a critical frequency that separates these two regimes and depends upon the field strength, particle magnetization, particle size, and fluid viscosity. By systematically changing these key variables, we verify the proposed theory through experimental investigation of the alignment behavior of these particle systems.

Theory

When the magnetic field is rotating at sufficiently low frequencies, magnetically responsive platelets are dominated by magnetic torque and will roll along a substrate surface synchronously with the rotating field (phase-locked). At higher frequencies, however, viscous torque dominates and hinders the platelet from synchronous rotation. As a result, the platelets are forced to align parallel with the plane of the rotating magnetic field (phase-ejection), as illustrated in Fig. 1.

[a]*Complex Materials, Department of Materials, ETH Zurich, 8093 Zurich, Switzerland. E-mail: andre.studart@mat.ethz.ch*
[b]*Laboratory of Metal Physics and Technology, Department of Materials, ETH Zurich, 8093 Zurich, Switzerland*
[c]*Earth and Planetary Magnetism, Department of Earth Sciences, ETH Zurich, 8092 Zurich, Switzerland*
† Electronic supplementary information (ESI) available. See DOI: 10.1039/c2sm25650a

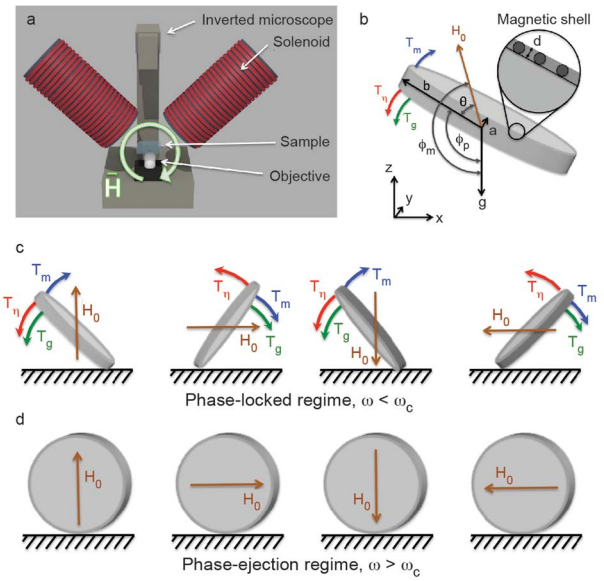

Fig. 1 (a) Experimental setup used to investigate the non-linear alignment dynamics of platelets under a rotating magnetic field, H_0. (b) Schematic diagram of a magnetically labeled platelet in an external magnetic field. The magnetic nanoparticles used for labeling are indicated on the surface of the nonmagnetic platelet. (c) Torques exerted on a platelet rolling along a substrate in the phase-locked regime. (d) In the phase-ejection regime, the field is rotating too fast for synchronous rotation, causing the platelet to flip parallel to the field rotation. Here, the magnetic field is rotating in the x–z plane (T_m = magnetic torque, T_η = viscous torque, and T_g = gravitational torque).

To determine the critical frequency at which this transition occurs, we solve a torque balance equation that takes into account the magnetic, gravitational, and viscous torques acting on the nonmagnetic platelets coated with iron oxide nanoparticles.

The magnetic nanoparticles inhabit a thin shell volume around the perimeter of the platelet that is as thick as the diameter of the nanoparticle, d = 12 nm (Fig. 1b). The magnetic susceptibility of this particle shell, χ_{ps}, is dependent on the susceptibility of the nanoparticles, χ_{np}, and their packing fraction in the shell, φ_{np}, as $\chi_{ps} = \chi_{np}\varphi_{np}$. The magnetic torque, T_m, exerted on those particles in the presence of an external magnetic field is given by the derivative of the magnetic energy, U_{ps}, with respect to the angle θ between the platelet's long axis and the applied field (Fig. 1b). The magnetic energy of a shell of magnetic material can be calculated analytically by assuming an ellipsoidal geometry as[5]

$$U_{ps} = -\frac{2\pi\mu_0\chi_{ps}^2}{3(\chi_{ps}+1)}\left[(a+d)(b+d)^2 - ab^2\right]H_0^2\sin^2\theta, \quad (1)$$

where a and b are half the thickness and half the diameter of the platelet, respectively, μ_0 is the magnetic permeability of free space, H_0 is the external field, and θ represents the phase lag of the platelet. The phase lag, θ, equals $\phi_m - \phi_p$, where ϕ_m and ϕ_p are the angles between the magnetic field vector and the platelet's long axis, respectively, with respect to the gravitational vector, g (Fig. 1b). Differentiating $-U_{ps}$ with respect to θ yields the following expression for the magnetic torque:

$$T_m = \frac{2\pi\mu_0\chi_{ps}^2}{3(\chi_{ps}+1)}\left[(a+d)(b+d)^2 - ab^2\right]H_0^2\sin^2\theta \quad (2)$$

Considering only magnetic torque, the platelet will be driven towards alignment with the magnetic field ($\theta = 0$), at which point the magnetic torque approaches 0. However, under rotation the platelet experiences a viscous (frictional) torque that opposes rotation and creates a phase lag ($\theta > 0$). This viscous torque, T_η, is proportional to the angular frequency of the platelet, $d\phi_p/dt$, and the viscosity of the surrounding fluid, η, as

$$T_\eta = -6\eta V_p(d\phi_p/dt)(f/f_0), \quad (3)$$

where f/f_0 represents the Perrin friction factor, the ratio between the friction of a rolling ellipse compared to a rolling sphere of equal volume V_p,[9] where in our case $V_p = 2\pi ab^2$. Perrin friction factors can be readily solved for ellipsoidal geometries rolling end over end, derived previously[9] as

$$\frac{f}{f_0} = \frac{4}{3}\frac{1-p^2}{(2-p^2aS)}, \quad (4)$$

where

$$S = (2/a)(p^2-1)^{-1/2}\tan^{-1}\left[(p^2-1)^{1/2}\right].$$

Here, p is the aspect ratio of the platelet, b/a. As the platelet rotates at low frequencies, it is pushed out-of-phase with respect to the magnetic field by the viscous torque. The platelet finds a stable phase lag behind the magnetic field, where the magnetic torque balances with the viscous torque (Fig. 1c).

Finally, as the platelets roll along the surface, gravitational torque also needs to be considered. The gravitational torque will always work to flatten the platelets in-plane due to sedimentation either in the bulk fluid or onto the substrate. The gravitational contributions can either work to add to ($\phi_p > 180°$), or subtract from ($\phi_p < 180°$), the magnetic torque. This means that at a fixed magnetic field angular frequency, ($d\phi_m/dt$), the velocity of the platelet is not static, but instead fluctuates slightly due to the current gravitational contribution. However, for the magnetic fields studied here, ($H_0 > 50$ Oe), these gravitational contributions are typically two or more orders of magnitude smaller than the magnetic and viscous contributions and thus have been disregarded.

For particles rolling in a steady state, there must be a net balance of torques with respect to the moving axis of the field such that $T_m + T_\eta = 0$. Inserting eqn (2) and (3) into this torque balance and rewriting the particle rotation in terms of the phase-lag generates the following expression:

$$\frac{d\theta}{dt} = \omega - \omega_c\sin 2\theta, \quad (5)$$

with

$$\omega_c = \frac{\mu_0\chi_{ps}^2H_0^2}{18(f/f_0)\eta(\chi_{ps}+1)}\left[\frac{(a+d)(b+d)^2}{ab^2} - 1\right].$$

Here, the rotation of the field is written in terms of the field frequency, ω, where $\omega = d\phi_m/dt$. When the particle is phase-locked with the external magnetic field, the phase does not

change in time ($d\theta/dt = 0$), provided we disregard the gravitational contributions. According to eqn (5), this is only possible if ω is lower than the critical value of ω_c. This critical frequency defines the regime where the platelets abruptly change from phase-locked behavior to phase-ejection (Fig. 1d). If magnetic rolling of platelets in suspension is desired, then the external magnetic field must be rotated slower than the critical frequency. Instead, if alignment control over two axes of the platelet is desired, this rotation must exceed the critical frequency. Eqn (5) parallels the equation of motion of an overdamped non-linear oscillator, which has been used to describe other rotational[10] and translational[11,12] dynamics of colloidal particles.

Experimental methods

To test the theoretical model proposed in eqn (5), describing the dynamics of nonmagnetic platelets coated with magnetic nanoparticles, we designed a series of experiments which systematically varied some of the parameters affecting the critical frequency, ω_c (eqn (5)). Aluminum oxide platelets with an average long-axis diameter of 7.5 μm and 200 nm thickness were used in all experiments (Alusion®, Antaria, Bentley, Australia). In each case, platelets were coated with iron oxide nanoparticles and suspended in poly(vinyl alcohol) (PVA) solutions. Specifically, 0.5 g of platelets was first suspended in 20 ml of deionized water at pH = 7. Under continuous stirring, a range of μl volumes of EMG-705 Ferrofluid (Ferrotec, Germany) diluted with 5 ml of deionized water was added drop by drop. The EMG-705 ferrofluid is an aqueous suspension containing 3.6 wt% of iron oxide nanoparticles coated with an anionic surfactant. At pH = 7, the alumina platelets have a positive surface charge, causing the iron oxide nanoparticles coated with anionic surfactant to electrostatically adsorb on the platelet surface. When the liquid phase of the suspension became transparent, the adsorption of the iron oxide was considered complete. The coated platelets were then rinsed with deionized water three times, by letting them sediment to the bottom of a glass vial and repeatedly changing the supernatant solution. Subsequently, the magnetized platelets were dried for 12 hours at 80 °C. The magnetized alumina platelets were investigated with a scanning electron microscope. As seen in Fig. 2a and b, the surface coverage of iron oxide nanoparticles was found to be homogeneous. As such, surface coatings were calculated geometrically, assuming complete and homogeneous absorption of all nanoparticles onto the alumina platelets.

To measure the magnetic susceptibility of the resulting platelets, 210 mg of platelets was mixed into 1 ml of triethylene glycol dimethacrylate (TEGDMA, Sigma-Aldrich) with 0.5 wt% camphorquinone (Sigma-Aldrich) and 0.5 wt% ethyl-4-dimethylaminobenzoate (Sigma-Aldrich). The resulting suspensions were poured into cylindrical molds subjected to a horizontal 1 Hz rotating magnetic field applied to align the magnetized platelets horizontally in the upright cylinder mold. After 10 s, the solutions were polymerized using a Bluephase 20i curing light (Ivoclar Vivadent, Liechtenstein). The magnetic susceptibilities of the aligned samples were then measured in both parallel and perpendicular orientations using a field amplitude of 10 Oe at a frequency of 1 kHz and at room temperature in a Quantum Design Physical Property Measurement System (PPMS), equipped with a 9 T magnet.

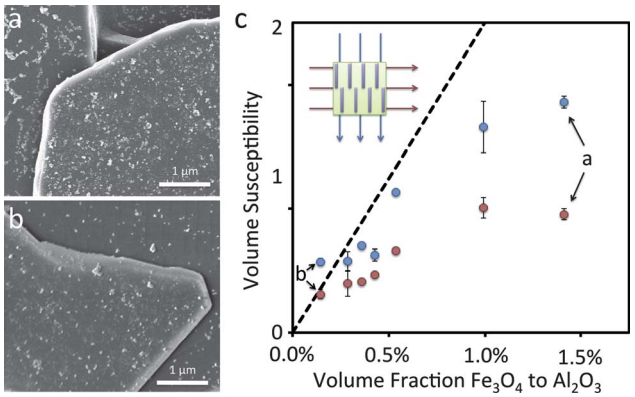

Fig. 2 Scanning electron micrograph of iron-oxide-coated platelets at (a) 1.43 and (b) 0.14 vol% Fe_3O_4. (c) Volume magnetic susceptibility measurements of TEGDMA matrices loaded with alumina platelets with varying surface coverage of iron oxide nanoparticles relative to the volume of an alumina platelet. Blue and red dots indicate susceptibility measurements with parallel and perpendicular platelets, respectively. The black dotted line is the theoretical susceptibility for equivalent volumes of homogeneous, non-interacting iron oxide nanoparticles.

Fluid cells were set up to allow controlled testing of the magnetic response of the alumina platelets when suspended in liquids. Liquids of various viscosities were prepared by dissolving different concentrations of poly(vinyl alcohol) powder (PVA, Sigma-Aldrich, molar mass = 13 000–23 000 g mol^{-1}) in deionized water. The dynamic viscosities of the PVA solutions were calculated from the kinematic viscosity measured using an Ostwald viscometer. Fluid viscosities between 1 and 42 mPa s could be obtained by dissolving up to 16 wt% of PVA in water. In a typical experiment, ~20 mg of magnetized alumina platelets were added to 1 ml of PVA solution and vortex mixed for 1 minute. A 10 μl droplet of sample suspension was placed in a fluid cell consisting of a Secure-Seal Imaging Spacer (SS8X9, Grace Bio-Labs, USA), sandwiched between a glass coverslip and a bottom 100 μm thick, transparent Teflon foil taped to a glass microscope slide for support.

The rotating field setup was constructed around a DMIL LED inverted light microscope (Leica Microsystems GmbH, Germany). Two solenoids were arranged perpendicular to each other and positioned in the x–z plane to allow easy observation of the sample (Fig. 1a). The strength of the applied alternating fields and the frequency of the alternation were computer-controlled using LabView (National Instruments, USA) and amplified using two BOP 20-5M power amplifiers (KEPCO, USA). To create a rotating field, the sinusoidal currents applied to the two solenoids were offset by 90°. The frequency of the field was programmed to increase exponentially with time to allow easy determination of the critical frequency. The fluid cell was placed in the center of these solenoids, which was directly above the objective of the microscope.

Using this setup, we were able to take videos, normally with a 10× objective, to observe the platelet alignment as a function of time and therefore frequency. The videos obtained were analyzed manually to determine the phase ejection point, which corresponds to the time when 50% of the particles are phase-ejected.

For each system considered, five videos with around 100 platelets in the field of view were produced and statistically evaluated.

Results and discussion

The measured magnetic susceptibility of polymer samples loaded with platelets coated with different iron oxide concentrations is shown in Fig. 2c. Using a susceptibility of the iron oxide nanoparticles of $\chi_{np} = 21$ previously measured for these particles in solution,[2] we obtain theoretical susceptibilities of the platelet-loaded polymer samples from the relation $\chi_{ps} = \chi_{np}C_{np}$, where C_{np} is the volume fraction of iron oxide nanoparticles within the polymer sample. A treatment of this type represents a hypothetical case where the iron oxide nanoparticles are homogeneously distributed throughout the platelet-loaded polymer. Such theoretical susceptibilities are indicated by the dashed black line in Fig. 2c. We find that for iron oxide fractions of below 0.5 vol%, the measured values for the magnetic susceptibility of polymer samples, containing magnetized platelets oriented parallel to the magnetic field, are predicted reasonably well using the homogeneous approximation. For samples containing perpendicular platelets, the constrained 2-D positioning of the magnetic nanoparticles on the platelet surfaces that oppose the applied magnetic field could lead to unfavorable superparamagnetic "blocking". The "blocking" effect arises when the magnetic dipoles of adjacent nanoparticles interact with each other such that the dipoles are no longer completely free to change their orientations in response to external fields. Indeed, nanoparticles in perpendicular configurations generate a slightly lower magnetic response compared to the parallel configurations (Fig. 2c), suggesting that full alignment of magnetic dipoles in the direction of the external magnetic field is not possible in the former case. Because of the closer proximity between nanoparticles, blocking effects are more likely to occur at high volume fractions of iron oxide. This explains the stronger deviation between the experimental data and the homogeneous approximation for iron oxide concentrations greater than 0.5 vol% (Fig. 2c). A similar geometry-constrained blocking effect showcasing a parallel configuration is perhaps best exemplified in magnetotactic bacteria where the magnetic nanoparticles are confined in 1-D chain structures. In this case the "blocking" effect works to increase the assembly's susceptibility, since the 1D confinement leads to interparticle interactions that favor alignment of dipoles parallel with the external magnetic fields. As a result, superparamagnetic blocking occurs at smaller particle diameters in this biological system.[13] In the 2-D constrained geometry investigated here, both parallel and anti-parallel arrangements of the dipoles of adjacent nanoparticles are possible when the platelets are aligned parallel to the field. Since the probability of finding one or the other arrangement is the same, the moments of the interacting dipoles approximately cancel out. This is presumably why the experimental measurements in this case can be approximated by the homogeneous solution. For platelets aligned perpendicular to the field, anti-parallel arrangements are more likely to occur. This is probably the reason for the lower magnetic susceptibility measured in this case.

When the magnetized platelets are subjected to rotating magnetic fields at frequencies below the critical frequency, they exhibit the phase-locked rolling behavior predicted (Fig. 3a–c and Movie S1†). In contrast, at higher frequencies, the magnetized platelets experience phase ejection and orient their long axes in-line with the plane of the rotating field (Fig. 3e). The intermediate frequencies generate a transition regime where individual platelets are either phase-locked or phase-ejected (Fig. 3d). This transition regime spans a relatively wide frequency range (Fig. 3f) because of the polydispersity of the platelet sizes (4–20 μm). Monodisperse platelets would exhibit a step-function in the phase transition, indicating that all platelets align at the same critical frequency. Platelets rolling near a substrate will also experience translation in the direction of rolling motion. This translation is reversed if the rotating field is reversed and reduced for platelets further from the substrate.

While the phase transition for individual platelets occurs abruptly at the critical frequency, interesting phenomena were also observed for a few of the imaged platelets. First, some platelets underwent wobbling near the critical frequency (Movie S2†). In this case the platelets appear to sample both the phase-locked and phase-ejection regimes. As this does not occur for many platelets, it appears that the effect occurs only for specific geometries or magnetite coatings. Second, above the critical frequency, some platelets were observed to be spinning as a wheel, instead of rolling end-over-end (Movie S3†). This behavior suggests that the platelets have a preferred axis of magnetization or a specific easy-axis. This secondary rolling should exhibit a secondary critical frequency that can be overcome to stop the behavior. The spinning may cause concentration gradients over very long timescales if desired, but generally plays a minimal role in the subsequent implementation of the above technique.

Despite the platelet polydispersity, reliable trends in the critical frequency have been determined as shown in Fig. 4. The experimental results obtained for magnetite concentrations around 0.5 vol% provide reasonable agreement with eqn (5), which predicts a linear dependence of the critical frequency on the inverse of the viscosity, the square of the applied magnetic

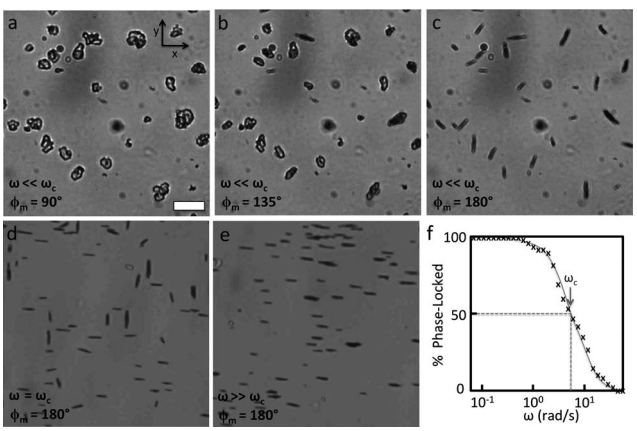

Fig. 3 Experimental micrographs showing the platelets in (a–c) the phase-locked regime, (d) a transition regime, and (e) the phase-ejection regime. Scale bar, 20 μm. (f) Plot of the percentage of platelets in the phase-locked regime. Symbols are experimental points and the line is a guide for the eyes. Here, the field is rotated in the x–z plane, $\chi_p = 1.33$, $\eta = 1.34$ mPa s, and $H_0 = 100$ Oe.

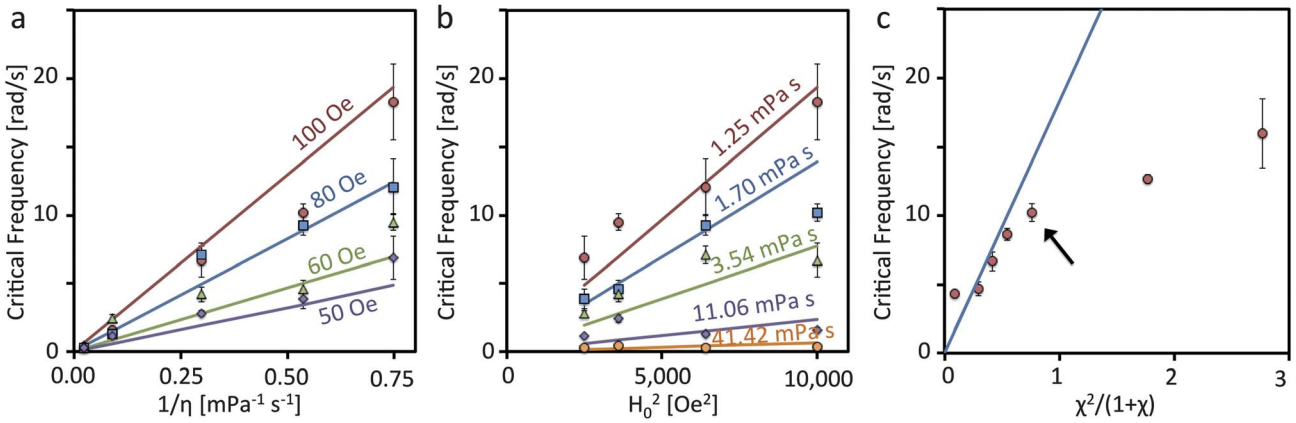

Fig. 4 Plots of the critical frequency *versus* (a) the inverse of viscosity, $1/\eta$; (b) the square of the magnetic field strength, H_0^2; and (c) the susceptibility fraction relation, $\chi^2/(1+\chi)$. Data shown in (a) and (b) were obtained for platelets with a Fe_3O_4 volume fraction of 0.53% with the susceptibility indicated by the black arrow in (c). Experimental points (symbols) show good agreement with theoretical predictions (lines) using a Perrin friction factor of 16.46 for all data.

field strength, and the susceptibility fraction relation, $\chi^2/(1+\chi)$. The deviation between prediction and experimental results for magnetite concentrations above 0.5 vol% (Fig. 4c) may be a result of the magnetic blocking effects mentioned previously. All data can be plotted further on a universal curve (Fig. 5a) that shows a clear trend between experimental critical frequencies and the term $\chi_{ps}^2 H_0^2/(\chi_{ps}+1)\eta$, as expected from eqn (5).

To further test the validity of eqn (5) in describing the dynamics of our magnetized platelets, we compare the constant friction factors obtained from the experimental data (Fig. 4) with the theoretical Perrin friction factor, ffl_0, of 16.46 calculated for oblate spheroids with the same aspect ratio as the platelets. Experimental friction factors calculated from best-fits to eqn (5) generate a mean value of 15.5, which is in very good agreement with the theoretical estimate. Our ability to predict the alignment dynamics of magnetized platelets using eqn (5) allows us to determine *a priori* the minimum frequency required to obtain composites with high volume fractions of bi-axially oriented reinforcing platelets.

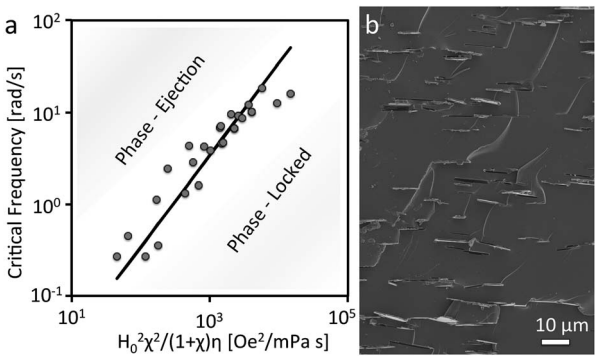

Fig. 5 (a) Universal curve showing the dependence of the critical frequency on magnetic field strength, magnetic susceptibility and fluid viscosity. The black line shows the theoretical prediction using a Perrin friction factor of 16.46. (b) Composite material consisting of 5 vol% bi-axially aligned alumina platelets ($\chi_p = 1.33$) in a TEGDMA matrix that was light-cured while exposed to a 1 Hz, 100 Oe rotating magnetic field.

Composites containing alumina platelets oriented using rotating magnetic fields were prepared to further demonstrate the usability of this model. Magnetized platelets could be aligned bi-axially in a 100 Oe rotating magnetic field, provided that the field frequency was sufficiently higher than the critical value predicted by eqn (5). As the viscosity of the TEDGMA monomer solution used in this case is around 40 mPa s, a rotating field of 1 Hz was used, which is higher than the critical frequency of 0.6 Hz estimated from eqn (5). Fig. 5 shows the resulting polymerized methacrylate matrix exhibiting pronounced 2-D alignment of the platelets.

Conclusions

We offer a theoretical analytical model to describe the alignment dynamics of non-magnetic platelets coated with super-paramagnetic nanoparticles. Predictions for the critical frequency at which disk-shaped particles change from phase-locked rolling to phase-ejection were experimentally verified for a broad range of parameters, including platelet magnetization, fluid viscosity, and external magnetic field strength. Bearing these dependences in mind, we demonstrate the manufacturing of a polymer composite with a unique bi-axial orientation of reinforcing alumina platelets.

Acknowledgements

We thank Roman Ehrbar for his assistance with the experimental setup and Dr John Robinson (Antaria, Bentley, Australia) for providing the alumina platelets.

Notes and references

1 A. T. Skjeltorp, *Phys. Rev. Lett.*, 1983, **51**, 2306–2309.
2 R. M. Erb, H. S. Son, B. Samanta, V. M. Rotello and B. B. Yellen, *Nature*, 2009, **457**, 999–1002.
3 C. Ooi, R. M. Erb and B. B. Yellen, *J. Appl. Phys.*, 2008, **103**, 07E910.
4 J. Yuan, H. Gao, F. Schacher, Y. Youyong, R. Richter, W. Tremel and A. H. E. Müller, *ACS Nano*, 2009, **3**, 1441–1450.
5 R. M. Erb, R. Libanori, N. Rothfuchs and A. R. Studart, *Science*, 2012, **335**, 199–204.

6 S. B. Bubenhofer, E. K. Athanassiou, R. N. Grass, F. M. Koehler, M. Rossier and W. J. Stark, *Nanotechnology*, 2009, **20**, 485302.
7 D. van der Beek, A. V. Petukhov, P. Davidson, J. Ferré, J. P. Jamet, H. H. Wensink, G. J. Vroege, W. Bras and H. N. W. Lekkerkerker, *Phys. Rev. E: Stat., Nonlinear, Soft Matter Phys.*, 2006, **73**, 041402.
8 P. Tierno, J. Claret, F. Sagués and A. Cebers, *Phys. Rev. E: Stat., Nonlinear, Soft Matter Phys.*, 2009, **79**, 021501.
9 F. Perrin, *J. Phys. Radium*, 1934, **7**, 497–511.
10 B. H. McNaughton, K. A. Kehbein, J. N. Anker and R. Kopelman, *J. Phys. Chem. B*, 2006, **110**, 18958–18964.
11 B. B. Yellen, R. M. Erb, H. S. Son, R. Hewlin, Jr, H. Shang and G. U. Lee, *Lab Chip*, 2007, **7**, 1681–1688.
12 A. Cebers and M. Ozols, *Phys. Rev. E: Stat., Nonlinear, Soft Matter Phys.*, 2006, **73**, 021505.
13 R. Blakemore, *Science*, 1975, **190**, 377–379.

Addition and correction

Note from RSC Publishing

This article was originally published with incorrect page numbers. This is the corrected, final version.

The Royal Society of Chemistry apologises for these errors and any consequent inconvenience to authors and readers.